Article

Isolation and Structural Characterization of Capistruin, a Lasso Peptide Predicted from the Genome Sequence of Burkholderia thailandensis E264

Thomas A. Knappe, Uwe Linne, Se#verine Zirah, Sylvie Rebuffat, Xiulan Xie, and Mohamed A. Marahiel

J. Am. Chem. Soc., **2008**, 130 (34), 11446-11454 • DOI: 10.1021/ja802966g • Publication Date (Web): 01 August 2008

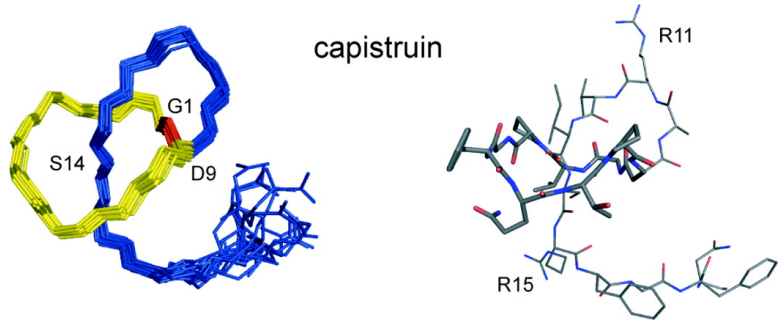

More About This Article

Additional resources and features associated with this article are available within the HTML version:

- Supporting Information
- Links to the 2 articles that cite this article, as of the time of this article download
- Access to high resolution figures
- Links to articles and content related to this article
- Copyright permission to reproduce figures and/or text from this article

View the Full Text HTML

J|A|C|S
ARTICLES

Published on Web 08/01/2008

Isolation and Structural Characterization of Capistruin, a Lasso Peptide Predicted from the Genome Sequence of *Burkholderia thailandensis* E264

Thomas A. Knappe,[†] Uwe Linne,[†] Séverine Zirah,[‡] Sylvie Rebuffat,[‡] Xiulan Xie,[†] and Mohamed A. Marahiel*[,†]

Department of Chemistry, Philipps-University Marburg, Hans-Meerwein-Strasse, D-35032 Marburg, Germany, and Chimie et Biochimie des Substances Naturelles, UMR 5154 CNRS, Muséum National d'Histoire Naturelle, CP 54, 57 rue Cuvier, 75005 Paris, France

Received April 22, 2008; E-mail: marahiel@chemie.uni-marburg.de

Abstract: Lasso peptides are a structurally unique class of bioactive peptides characterized by a knotted arrangement, where the C-terminus threads through an N-terminal macrolactam ring. Although ribosomally synthesized, only the gene cluster for the best studied lasso peptide MccJ25 from *Escherichia coli* consisting of the precursor protein McjA and the processing and immunity proteins McjB, McjC, and McjD is known. Through genome mining studies, we have identified homologues of all four proteins in *Burkholderia thailandensis* E264 and predicted this strain to produce a lasso peptide. Here we report the successful isolation of the predicted peptide, named capistruin. Upon optimization of the fermentation conditions, mass spectrometric and NMR structural studies proved capistruin to adopt a novel lasso fold. Heterologous production of the lasso peptide in *Escherichia coli* showed that the identified genes are sufficient for the biosynthesis of capistruin, which exhibits antimicrobial activity against closely related *Burkholderia* and *Pseudomonas* strains. In general, our rational approach should be widely applicable for the isolation of new lasso peptides to explore their high structural stability and diverse biological activity.

Introduction

Among the rapidly growing class of bioactive secondary metabolites from bacteria, many molecules are biosynthesized through a cyclization process.[1] The introduction of an intramolecular covalent linkage decreases dramatically the number of possible conformations and therefore entropically favors the specific interaction with the receptor protein and also provides protection against degradation by proteases.[2] Macrocyclic structures in bacteria are generated (I) by post-translational processing of ribosomally synthesized precursor proteins,[3−5] (II) by thioesterase-mediated cyclization of linear acyl chain precursors that are generated by nonribosomal peptide synthetases (NRPS) or polyketide synthases (PKS),[6,7] or (III) by ATP-dependent enzymatic macrocyclization of nonribosomally synthesized precursors as reported for desferrioxamine biosynthesis.[8] Within the class of ribosomal origin, lasso peptides are structurally unique and functionally diverse. They comprise 16−21 amino acids and share a complex three-dimensional structure.[9−17] An intramolecular cyclization reaction involving the α-NH_2 group of an N-terminal Gly/Cys residue and the side chain carboxyl group of a Glu/Asp residue at position 8 or 9 results in the formation of a macrolactam ring. The C-terminal tail of the peptide is threaded through the ring and irreversibly trapped by steric hindrance, forming the rigid lasso structure. Lasso peptides are classified depending on the presence (class I) or absence (class II) of four conserved cysteine residues which are involved in the formation of two intramolecular disulfide bonds.[4] Most of the currently known lasso peptides were isolated from Actinobacteria and act as enzyme inhibitors or receptor antagonists.[10−14]

[†] Philipps-University Marburg.
[‡] Muséum National d'Histoire Naturelle.

(1) Craik, D. J.; Daly, N. L.; Saska, I.; Trabi, M.; Rosengren, K. J. *J. Bacteriol.* **2003**, *185*, 4011–4021.
(2) Rizo, J.; Gierasch, L. M. *Annu. Rev. Biochem.* **1992**, *61*, 387–418.
(3) Willey, J. M.; van der Donk, W. A. *Annu. Rev. Microbiol.* **2007**, *61*, 477–501.
(4) Rebuffat, S.; Blond, A.; Destoumieux-Garzon, D.; Goulard, C.; Peduzzi, J. *Curr. Protein Pept. Sci.* **2004**, *5*, 383–391.
(5) Duquesne, S.; Destoumieux-Garzon, D.; Peduzzi, J.; Rebuffat, S. *Nat. Prod. Rep.* **2007**, *24*, 708–734.
(6) Fischbach, M. A.; Walsh, C. T. *Chem. Rev.* **2006**, *106*, 3468–3496.
(7) Kopp, F.; Marahiel, M. A. *Nat. Prod. Rep.* **2007**, *24*, 735–749.
(8) Kadi, N.; Oves-Costales, D.; Barona-Gomez, F.; Challis, G. L. *Nat. Chem. Biol.* **2007**, *3*, 652–656.
(9) Iwatsuki, M.; Tomoda, H.; Uchida, R.; Gouda, H.; Hirono, S.; Omura, S. *J. Am. Chem. Soc.* **2006**, *128*, 7486–7491.
(10) Katahira, R.; Yamasaki, M.; Matsuda, Y.; Yoshida, M. *Bioorg. Med. Chem.* **1996**, *4*, 121–129.
(11) Kimura, K.; Kanou, F.; Takahashi, H.; Esumi, Y.; Uramoto, M.; Yoshihama, M. *J. Antibiot.* **1997**, *50*, 373–378.
(12) Wyss, D. F.; Lahm, H. W.; Manneberg, M.; Labhardt, A. M. *J. Antibiot.* **1991**, *44*, 172–180.
(13) Katahira, R.; Shibata, K.; Yamasaki, M.; Matsuda, Y.; Yoshida, M. *Bioorg. Med. Chem.* **1995**, *3*, 1273–1280.
(14) Frechet, D.; Guitton, J. D.; Herman, F.; Faucher, D.; Helynck, G.; Monegier du Sorbier, B.; Ridoux, J. P.; James-Surcouf, E.; Vuilhorgne, M. *Biochemistry* **1994**, *33*, 42–50.
(15) Rosengren, K. J.; Clark, R. J.; Daly, N. L.; Goransson, U.; Jones, A.; Craik, D. J. *J. Am. Chem. Soc.* **2003**, *125*, 12464–12474.
(16) Wilson, K. A.; Kalkum, M.; Ottesen, J.; Yuzenkova, J.; Chait, B. T.; Landick, R.; Muir, T.; Severinov, K.; Darst, S. A. *J. Am. Chem. Soc.* **2003**, *125*, 12475–12483.
(17) Bayro, M. J.; Mukhopadhyay, J.; Swapna, G. V.; Huang, J. Y.; Ma, L. C.; Sineva, E.; Dawson, P. E.; Montelione, G. T.; Ebright, R. H. *J. Am. Chem. Soc.* **2003**, *125*, 12382–12383.

 10.1021/ja802966g CCC: $40.75

A typical class II lasso peptide and the best studied representative is microcin J25 (MccJ25),[15−17] which is synthesized and secreted by *Escherichia coli* AY25.[18] The antibacterial MccJ25 enters bacteria using the iron siderophore receptor FhuA[19] and inhibits RNA polymerase by binding within the NTP uptake channel.[20] The macrolactam ring of MccJ25 results from an amide bond between Gly_1 and Glu_8, and the C-terminal tail is sterically entrapped in the ring by the two bulky side chains of Phe_{19} and Tyr_{20}.[15−17] Among all known lasso peptides, only the genetic determinants for the production of MccJ25 are known. The *mcjABCD* gene cluster is necessary for MccJ25 biosynthesis.[21] The gene *mcjA* encodes a 58 amino acid precursor protein, whereas the terminal 21 amino acids are found in the bioactive lasso peptide. Proteins encoded by *mcjB* and *mcjC* are required for the production of MccJ25 and were sufficient to convert McjA into MccJ25 in vitro.[22,23] The gene *mcjD* is predicted to encode an ATP-binding cassette (ABC) transporter which is involved in the export of MccJ25 and concomitantly acts as an immunity protein.

Genome mining, in general, is a powerful method to explore natural product diversity and was proven to be useful to identify genetic loci that encode natural products with new biosynthetic potential.[24,25] Upon identification of interesting biosynthetic gene clusters by genome mining approaches and the identification of the synthesized metabolites, it is desirable to establish the expression of the entire gene cluster in a heterologous host benefiting from increased production levels and genetic accessibility. The heterologous biosynthesis of echinomycin, a nonribosomal peptide with antitumor activity,[26] and of the patellamides, ribosomally encoded peptides from an obligate (unculturable) cyanobacterial symbiont of *Lissoclinum patella*,[27] in *Escherichia coli* exemplifies this approach.

Burkholderia thailandensis E264 is a nonvirulent soil bacterium closely related to *Burkholderia pseudomallei* which causes melioidosis. It is nutritionally diverse and grows at temperatures ranging from 25 to 42 °C. Comprehensive analysis of microbial genomes displayed that *Burkholderia* strains reveal the genes for the production of many previously unknown NRPSs/PKSs[28] and are therefore a promising source for the isolation of natural products in general.

In this study, we have identified capistruin, a new lasso peptide from *Burkholderia thailandensis* E264. We predicted the primary structure of capistruin by genome mining approaches and were able to isolate the predicted molecule from culture supernatants. Mass spectrometric and NMR spectroscopic studies proved capistruin to be a new representative of lasso peptides. Furthermore, the heterologous production of capistruin in *E. coli* was established, and bioactivity assays revealed antibacterial activity against closely related strains.

Experimental Procedures

Strains and General Methods. *Burkholderia thailandensis* E264 was purchased from German Collection of Microorganisms and Cell Cultures (DSMZ). Oligonucleotides were purchased from Operon Biotechnologies. DNA dideoxy sequencing confirmed the identity of constructed plasmids.

Purification of Capistruin. *Burkholderia thailandensis* E264 was incubated at 37 °C overnight in LB medium containing gentamycin (8 μg mL^{-1}). Subsequently, M20 medium containing the same antibiotic was inoculated to an OD_{600} of 0.01 and incubated at 42 °C for 24 h. M20 medium is composed of 20 g/L L-glutamic acid, 0.2 g/L L-alanine, 1.0 g/L sodium citrate, 20 g/L disodium hydrogen phosphate, 0.5 g/L potassium chloride, 0.5 g/L sodium sulfate, 0.2 g/L magnesium chloride, 0.0076 g/L calcium chloride, 0.01 g/L iron(II) sulfate, and 0.0076 g/L manganese sulfate, pH 7.0. Cultures were harvested by centrifugation, and the combined supernatants were applied to solid phase extraction using Strata C8 cartridges. Upon loading of the supernatant, the resin was washed with water and eluted with 100% methanol. Eluate was evaporated to dryness, dissolved in 10% acetonitrile and finally applied onto a RP-HPLC preparative *Nucleodur* C18ec column (250 mm × 21 mm). Elution was performed applying the following gradient of water/0.05% formic acid (solvent A) and acetonitrile/0.045% formic acid (solvent B) at a flow rate of 18 mL min^{-1}: linear increase from 10% B to 40% B within 30 min followed by a linear increase to 95% B in 5 min and holding 95% B for additional 2 min. The retention time of capistruin was 25.8 min.

Mass Spectrometric Analysis. The mass spectrometric characterization of capistruin was performed with an LTQ-FT instrument (Thermo Fisher Scientific, Bremen, Germany) connected to a microbore 1100 HPLC system (Agilent, Waldbronn, Germany). Separation of extracted capistruin from contaminants was achievd using a 125/2 Nucleodur C18ec column (Macherey-Nagel, Düren, Germany) applying the following gradient of water/0.05% formic acid (solvent A) and acetonitrile/0.045% formic acid (solvent B) at a column temperature of 40 °C and a flow rate of 0.2 mL min^{-1}: linear increase from 10% B to 40% B within 30 min followed by a linear increase to 95% B in 5 min and holding 95% B for additional 2 min.

CID fragmentation studies within the linear ion trap were either done using online LCMS or utilizing purified capistruin samples. The purified samples were analyzed using a syringe pump at a flow rate of 10 μL min^{-1}. Usually, the doubly charged ions were selected for fragmentation in the ion trap since they were the dominant species in the spectrum. The energy for fragmentation was set to 35 in all cases.

Cloning of Capistruin Gene Cluster. The *capABCD* gene cluster was amplified from genomic DNA of *Burkholderia thailandensis* E264 by PCR using the forward primer (*Nde*I) GCACATATGGTTCGACTTTTGGCGAAGCTGCTTCGTTCGACG and the reverse primer (*Nco*I) ATACCATGGTCACGCCTTCGCGTCGGCGGGTTCGGG. PCR was carried out with DyNAzyme EXT DNA polymerase (New England Biolabs) following the instructions of the manufacturer for GC-rich and long DNA templates. The resulting amplicon was digested with *Nde*I and *Nco*I and cloned into pET-41a(+). Plasmids were analyzed by DNA sequencing and transformed into *E. coli* BL21(DE3) for heterologous synthesis of capistruin.

Heterologous Synthesis of Capistruin in *E. coli*. LB medium containing kanamycin (50 μg mL^{-1}) was inoculated with *E. coli* BL21(DE3) cells transformed with the pET-41a(+)_*capABCD* vector and grown at 37 °C overnight. M20 medium containing kanamycin (50 μg mL^{-1}), thiamine (2 μg mL^{-1}), biotin (2 μg

(18) Salomon, R. A.; Farias, R. N. *J. Bacteriol.* **1992**, *174*, 7428–7435.
(19) Destoumieux-Garzon, D.; Duquesne, S.; Peduzzi, J.; Goulard, C.; Desmadril, M.; Letellier, L.; Rebuffat, S.; Boulanger, P. *Biochem. J.* **2005**, *389*, 869–876.
(20) Mukhopadhyay, J.; Sineva, E.; Knight, J.; Levy, R. M.; Ebright, R. H. *Mol. Cell* **2004**, *14*, 739–751.
(21) Solbiati, J. O.; Ciaccio, M.; Farias, R. N.; Gonzalez-Pastor, J. E.; Moreno, F.; Salomon, R. A. *J. Bacteriol.* **1999**, *181*, 2659–2662.
(22) Duquesne, S.; Destoumieux-Garzon, D.; Zirah, S.; Goulard, C.; Peduzzi, J.; Rebuffat, S. *Chem. Biol.* **2007**, *14*, 793–803.
(23) Clarke, D. J.; Campopiano, D. J. *Org. Biomol. Chem.* **2007**, *5*, 2564–2566.
(24) Wilkinson, B.; Micklefield, J. *Nat. Chem. Biol.* **2007**, *3*, 379–386.
(25) Lautru, S.; Deeth, R. J.; Bailey, L. M.; Challis, G. L. *Nat. Chem. Biol.* **2005**, *1*, 265–269.
(26) Watanabe, K.; Hotta, K.; Praseuth, A. P.; Koketsu, K.; Migita, A.; Boddy, C. N.; Wang, C. C.; Oguri, H.; Oikawa, H. *Nat. Chem. Biol.* **2006**, *2*, 423–428.
(27) Schmidt, E. W.; Nelson, J. T.; Rasko, D. A.; Sudek, S.; Eisen, J. A.; Haygood, M. G.; Ravel, J. *Proc. Natl. Acad. Sci. U.S.A.* **2005**, *102*, 7315–7320.
(28) Minowa, Y.; Araki, M.; Kanehisa, M. *J. Mol. Biol.* **2007**, *368*, 1500–1517.

mL^{-1}), and IPTG (0.02 mM) was inoculated with the starter culture to an OD_{600} of 0.01 and cultivated at 37 °C for 48 h. Supernatant and extract obtained by described solid phase extraction were analyzed by LCMS using a high-resolution Fourier transform mass spectrometer.

NMR Spectroscopy. Samples for NMR measurements contained 4.4 mg of capistruin in 250 μL of H_2O/D_2O (9:1) at 283 K. Spectra were recorded on a Bruker Avance 600 MHz spectrometer equipped with an inverse probe with *z*-gradient. Samples were filled into Wilmad 3 mm tubes obtained from Rototec Spintec. Temperature effect on the structure was surveyed by recording ^1H spectra at variable temperatures (283, 288, 293, 298, 300 K). ^1H and TOCSY spectra were recorded in D_2O at 283 K sequentially 2 h, 1 day, and 10 days after sample preparation. For sequential assignment,[29] DQF-COSY, TOCSY, NOESY, ROESY, and ECOSY experiments[30] were performed in phase-sensitive mode using States-TPPI.[31] TOCSY spectra were recorded with mixing times of 50 and 80 ms. NOESY spectra were taken at 70, 100, 150, and 300 ms mixing times, while ROESY spectra at 200 ms were observed. Water suppression was fulfilled by using excitation sculpting[32] with gradients for DQF-COSY, TOCSY, NOESY, and ROESY experiments, while presaturation was used for ECOSY. One-dimensional spectra were acquired with 65 536 data points, while 2D spectra were collected using 4096 points in the F_2 dimension and 512 increments in the F_1 dimension. For 2D spectra, 32 transients were used, with an exception of 72 transients for ECOSY. Relaxation delay was 2.5 s. Chemical shifts were referenced to H_2O, which in turn was calibrated using 2,2-dimethyl-2-silapentane-5-sulfonate (DSS) as internal standard in a different sample. All spectra were processed with Bruker TOPSPIN 2.1. NOESY spectra were analyzed within the program Sparky.[33]

Structure Calculations. Cross-peaks of NOESY spectra recorded at 283 K with mixing times of 70 and 100 ms were integrated and calibrated, and distance constraints were derived using Sparky. On the basis of the measured $^3J_{HH\alpha}$ and the Karplus relations,[34] torsion angle ϕ can be determined. Stereospecific assignments of β-methylene protons were done by using $^3J_{\alpha\beta}$ coupling constants, measured from ECOSY experiment in D_2O, in combination with NOE strengths between NH and βHs.[35] These constraints were used in the simulated annealing protocol, and structure calculations were performed with the program CYANA 2.1.[36] The coordinates of a set of 15 lowest energy structures to represent the solution structure of capistruin have been submitted to the Biological Magnetic Resonance Data Bank (BMRB) and assigned the accession number 20014.

Antibacterial Assays. The antibacterial activity of capistruin was assessed by radial diffusion assays against *Burkholderia caledonica*, *B. caribensis*, *B. ubonensis*, *B. vietnamiensis*, *Pseudomonas aeruginosa* AT27853, *P. azotoformans*, *P. cremoricolorata*, *P. oryzihabitans*, *P. fulva*, *P. parafulva*, *P. straminea*, *E. coli* K12 MC4100, *E. coli* 363, *E. coli* W3110, *Klebsiella pneumoniae*, *Salmonella enterica* Enteritidis, *S. enterica* Paratyphi SL69, *S. enterica* Thyphimurium LT2, *Enterobacter cloacae*, *Erwinia carotovora*, *Aerococcus viridans*, *Bacillus megaterium*, and *Staphylococcus aureus*. A bacteria soft agar layer was prepared by inoculating 10 mL of M63 or trypticase soy broth (TSB) soft agar media (6.5 g/L agar) with 100−250 μL inoculum of bacteria in exponential growth phase to reach 10^7 cfu/mL. The bacterial suspension was deposited onto a 20 mL LB or TSB agar (15 g/L agar) layer on petri dishes. After solidification, MccJ25 (1 nmol) and capistruin (5 nmol) diluted in Milli-Q water were laid over the bacteria layer. After 16−24 h incubation at 25, 30, or 37 °C (depending on the strain growth conditions), plates were analyzed for the presence of inhibition halos.

The minimal inhibitory concentrations (MICs) of capistruin against *Burkholderia caledonica*, *B. caribensis*, *B. ubonensis*, *B. vietnamiensis*, and *E. coli* 363 were determined by liquid growth inhibition assays in sterile 96-well microplates using poor broth (PB) as growth medium. The peptide was serially 1/2 diluted in sterile Milli-Q water to give concentrations between 0.5 and 1000 μM. Ten microliter peptide solutions were added to a 90 μL culture of bacteria diluted in PB to OD_{620} 0.002−0.005. Each peptide concentration was tested in triplicate. Control wells contained the peptide in PB. After incubation of the microplates for 14 h at 30 °C (37 °C for *E. coli* 363), the absorbance at 595 nm of the assay mixture was determined and was corrected by subtracting the absorbance due to the peptide alone in PB. MICs were defined as the lowest peptide concentrations that caused 100% growth inhibition. Concentration of the peptide stock solution was determined by amino acid composition. The peptide was hydrolyzed at 110 °C under vacuum in the presence of 6 M HCI for 24 h. Amino acids were derivatized using *o*-phthalaldehyde and separated using a Waters Alliance 2695 separation module equipped with a Pickering Laboratories PCX 5200 postcolumn derivatization instrument and a Waters 2475 fluorescence detector.

Results

Genome Mining Reveals Biosynthetic Gene Cluster of the Lasso Peptide Capistruin. In microcin J25 biosynthesis, the two processing enzymes McjB and McjC are sufficient to convert the precursor protein McjA into mature and active MccJ25.[22,23] While McjC shows sequence similarity to asparagine synthethase B, McjB does not show any homology to known enzymes. On the basis of initial similarity studies, revealing homologues of McjB, McjC, and McjD in *Burkholderia thailandensis* E264,[22] we investigated the localization of these genes within the *B. thailandensis* chromosome (GenBank accession no. CP000086) in detail. By manual ORF search of the upstream flanking region of the McjB homologue CapB, we identified a 144 bp ORF coding for a putative lasso peptide precursor protein CapA, which had not been annotated so far (Figure 1, Table 1).

The putative *capA* gene encodes a 47 amino acid precursor, and we proposed the first 28 residues to represent a leader peptide and the C-terminal 19 amino acids to form the mature peptide. The 19 residue peptide fragment features an N-terminal Gly and an Asp at position 9 and therefore matches the general primary structure requirements of lasso peptides.[4] The bulky side chains of Phe_{16} and Phe_{18} were predicted to be involved in sterically entrapping of the C-terminal tail, as observed for Phe_{19} and Tyr_{20} in MccJ25.[15]

In order to reveal the production of the predicted lasso peptide, *B. thailandensis* E264 was cultivated in M9 minimal medium containing gentamycin (8 $\mu g\ mL^{-1}$) and arabinose (2 $g\ L^{-1}$) at 37 °C for 24 h, in analogy to MccJ25 production.[37] The supernatant was screened for the molecular mass of the predicted cyclic peptide by LCMS using a high-resolution Fourier transform mass spectrometer. Trace amounts of a compound showing the exact mass of the cyclic peptide searched

(29) Wüthrich, K. *NMR of Protein and Nucleic Acids*; Wiley: New York, 1986.
(30) Berger, S.; Braun, S. *200 and More NMR Experiments. A Practical Course*; Wiley-VCH Verlag: Weinheim, Germany, 2004.
(31) Marion, D.; Ikura, M.; Tschudin, R.; Bax, A. *J. Magn. Reson.* **1989**, *85*, 393–399.
(32) Hwang, T.-L.; Shaka, A. J. *J. Magn. Reson. A* **1995**, *112*, 275–279.
(33) Goddard, T. D.; Kneller, D. J. *Sparky 3*; University of California, San Francisco.
(34) Guntert, P.; Braun, W.; Billeter, M.; Wuthrich, K. *J. Am. Chem. Soc.* **1989**, *111*, 3997–4004.
(35) Wagner, G. *Prog. Nucl. Magn. Reson. Spectrosc.* **1990**, *22*, 101–139.
(36) Herrmann, T.; Guntert, P.; Wuthrich, K. *J. Mol. Biol.* **2002**, *319*, 209–227.
(37) Blond, A.; Peduzzi, J.; Goulard, C.; Chiuchiolo, M. J.; Barthelemy, M.; Prigent, Y.; Salomon, R. A.; Farias, R. N.; Moreno, F.; Rebuffat, S. *Eur. J. Biochem.* **1999**, *259*, 747–755.

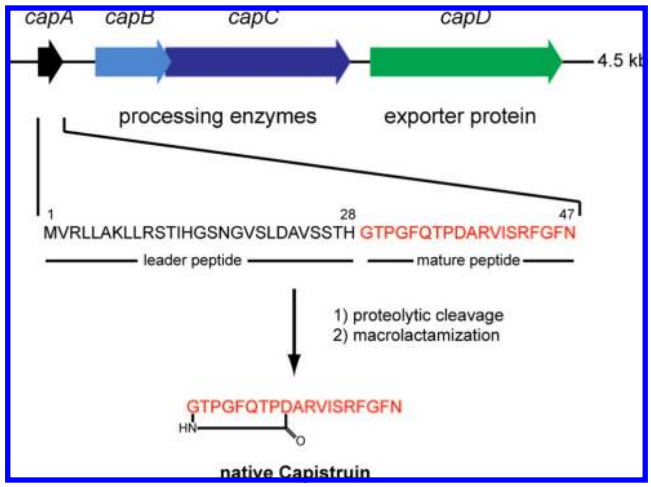

Figure 1. Capistruin biosynthetic gene cluster. The 19 amino acid mature peptide is excised from a 47 amino acid precursor protein encoded by *capA*. Genes involved in maturation (*capB* and *capC*) and export (*capD*) are coded downstream of *capA* on the chromosome of *B. thailandensis* E264.

Table 1. Coding Sequences from the Capistruin Biosynthetic Gene Cluster

protein	amino acids	proposed function	sequence similarity	overall identity/ similarity	GenBank accession no.
CapA	47	capistruin precursor protein			
CapB	221	protease	McjB	23%/36%	YP_442959.1
CapC	582	adenylation, cyclization	McjC	15%/38%	YP_442960.1
CapD	606	export, immunity protein	McjD	19%/44%	YP_442961.1

for $([M + 2H]^{2+}_{observed} = 1025{,}0206$; $[M + 2H]^{2+}_{calculated} = 1025{,}0191$, deviation 1.4 ppm) were detected (Figure 2a).

Mass Spectrometric Analysis. To determine if the compound was most likely a cyclic peptide, a branched cyclic peptide, or, as predicted, a lasso peptide, MS^n studies were performed using either a LTQ-FT or a QqTOF mass spectrometer. In general, cyclic peptides do not fragment extensively in MS^n experiments since more than one amide bond has to be broken in order to generate fragment ions. In the case of branched cyclic peptides, the linear part usually gives fragment ions in good yields, while the cyclic part does not. Mass spectrometric data previously published for the lasso peptide MccJ25 revealed a unique fragmentation behavior as fragments were observed where the C-terminus was noncovalently trapped within the ring.[15] In consideration of these different MS^n fragmentation behaviors, we performed gas phase fragmentation studies of the *m/z* 1025 doubly protonated species and found a very weak overall fragmentation. The most intense ions observed resulted from the loss of either water or ammonia, indicating a compact and rigid peptide structure. The remaining weak fragment ions present in the spectra (Figure 2b) arose from the C-terminal part of the peptide. Interestingly, all broken bonds identified are localized C-terminally to Arg_{11}. On the basis of these results, a head-to-tail cyclization could be excluded with high confidence. Since the only chemically possible branching point in this peptide was Asp_9, the question arose, why no fragmentation could be observed at the Asp_9-Ala_{10} and $Ala_{10}-Arg_{11}$ peptide bonds. To elucidate if the $[peptide_{1-10}]^+$ and $[peptide_{1-9}]^+$ b ions can also be formed in the gas phase, we performed MS^3 experiments with a linear ion trap mass spectrometer.

MS^3 studies of the *m/z* 1110.7 fragment ion (GTPGFQTPDAR; Figure 2c) allowed the additional cleavage of the C-terminal Arg_{11} and Ala_{10} residues. Not surprisingly, the remaining cyclic peptide could not be fragmented further in MS^4 experiments (data not shown). Supporting the compact structure of the peptide, no trypsin digestion was observed. Additionally, treatment with 1 M NaOH or incubation at 100 °C did not influence the peptide structure since the retention times and fragmentation spectra (including signal intensities) were identical to an untreated sample (data not shown).

In conclusion, the mass spectrometric results suggest a branched cyclic peptide with a rigid lasso structure. However, for the final structure elucidation, NMR experiments appeared to be necessary. For such studies, an optimized fermentation procedure for the production of milligram amounts was essential.

Influence of Growth Medium and Temperature on Lasso Peptide Production. In general, the production of secondary metabolites is strongly dependent on the growth conditions. To analyze this influence on lasso peptide production, we cultivated *B. thailandensis* E264 in different media and at different temperatures (Figure 3).

We observed that cultivation in M20 medium at 42 °C for 24 h increased the production by ~300-fold compared to our initial screening conditions (M9 medium, 0.2% arabinose, 37 °C, 24 h). Interestingly, the peptide was detectable even in the exponential phase of growth and was not limited to the early stationary phase, as observed for MccJ25[38] (Supporting Information Figure 1). On the basis of these findings and using an optimized purification protocol (as described in Experimental Procedures), capistruin could be purified with a yield of 0.7 mg/L culture, which facilitated further structural studies by NMR spectroscopy.

NMR Studies and Structure Determination of Capistruin. For the final structure elucidation, the lasso peptide was further characterized by NMR spectroscopy. A full assignment of ^1H signals was fulfilled (Supporting Information Table 1 and Figures 2 and 3). In the fingerprint region of the DQF-COSY spectrum (Supporting Information Figure 2), correlation was observed for each individual residue except Pro_3 and Pro_8. There are some minor correlations in the region (8.5−8.7 ppm/4.1−4.4 ppm) which do not correspond to the main conformation of capistruin and may be explained by the existence of a second minor conformation of the peptide under the experimental conditions. It is worth mentioning that strong sequential cross-peaks $H\alpha_i-H\delta_{i+1}$ in NOESY spectra were found for Pro_3 and Pro_8, which confirmed the two proline residues to be in the trans-conformation. Strong NOEs between NH of Gly_1 and the side chain protons of Asp_9 were observed, and this provided a direct evidence of an internal linkage between the α-NH_2 group of Gly_1 and the side chain carboxyl group of Asp_9 (Supporting Information Figure 3).

Additional long-range NOEs were observed between NH of Thr_2 and the side chain protons of Ser_{14}, Hα of Pro_3, and the side chain protons of Val_{12}, as well as Hα of Phe_5 and the side chain protons of Ile_{13}. Furthermore, NOEs between the NHs of both Gln_6 and Thr_7 with the side chain protons of Ile_{13}, Hα of Pro_8, and NH of Ser_{14}, and NH of Asp_9 and side chain protons of Ser_{14} were observed. All these long-range NOE contacts indicate a threading of the C-terminal tail of the peptide through the nine-residue ring and provide further evidence of the lasso structural motif. This novel lasso peptide was then designated capistruin.

(38) Chiuchiolo, M. J.; Delgado, M. A.; Farias, R. N.; Salomon, R. A. *J. Bacteriol.* **2001**, *183*, 1755–1764.

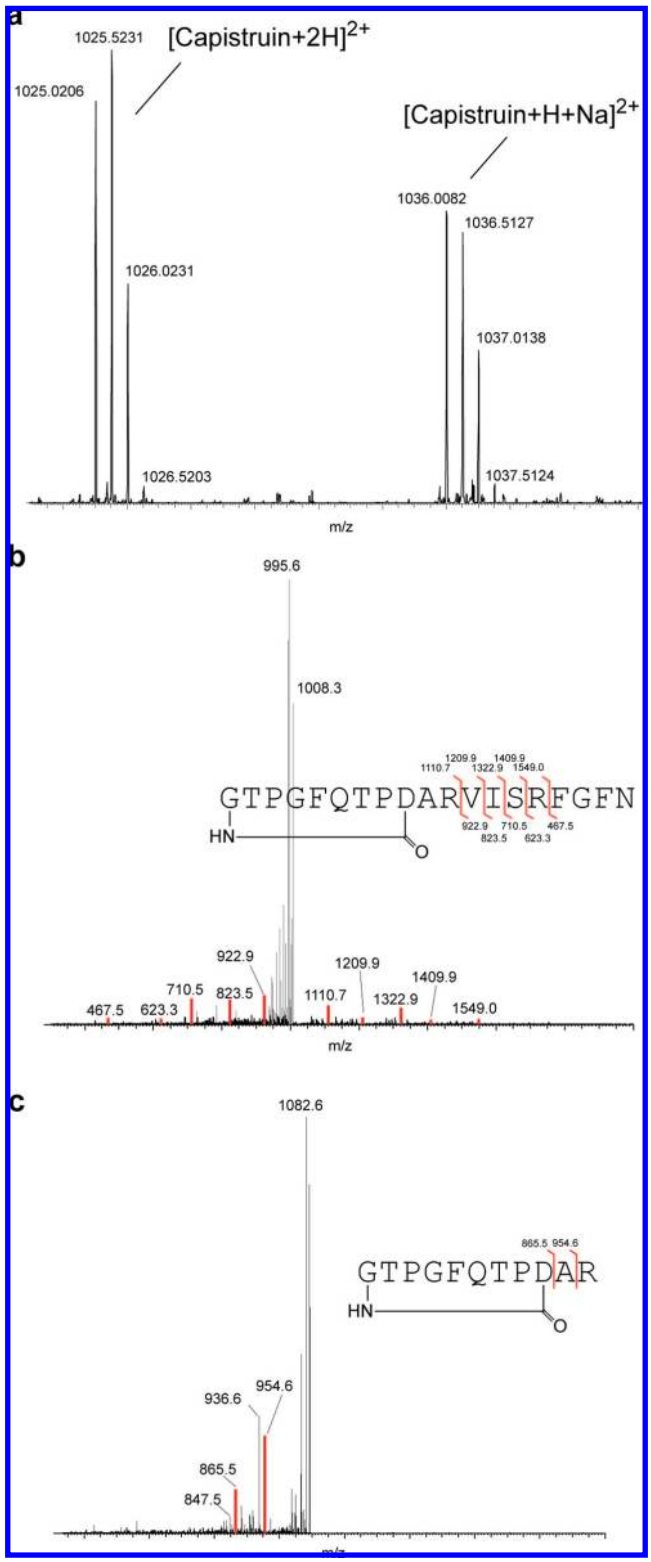

Figure 2. MS analysis of purified capistruin. (a) ESI-FT mass spectrum of capistruin is shown ($[M + 2H]^{2+}_{observed}$ = 1025,0206; $[M + 2H]^{2+}_{calculated}$ = 1025,0191, deviation 1.4 ppm). The peak at 1036 *m/z* corresponds to a sodium adduct. (b) MS^2 spectrum of the *m/z* 1025.0 doubly protonated precursor ion. The main signals (*m/z* 995.6 and 1008.3) correspond to the neutral loss of multiple molecules of water and/or ammonia since wide band activation was used. The peaks colored red represent the b and y ions shown schematically. (c) MS^3 spectrum of *m/z* 1110.7 $[capistruin_{1-11}]^+$. Schematic presentation of the red colored resulting fragments $[capistruin_{1-10}]^+$ and $[capistruin_{1-9}]^+$ is shown within the spectrum. The fragments were also observed with the additional loss of one molecule of water (−18) resulting in the *m/z* 936.6 and 847.5 fragment ions, respectively.

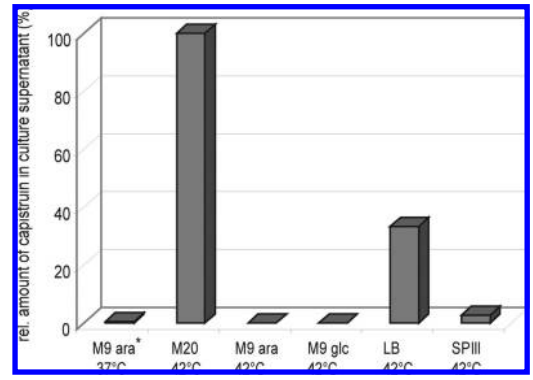

Figure 3. Growth medium dependent capistruin production of *Burkholderia thailandensis* E264. Relative amount of capistruin in the culture supernatant 24 h after inoculation derived from peak integration of extracted ion chromatograms. Initial identification conditions are labeled with an asterisk. Cultivation in M20 medium at 42 °C increases the production compared to the initial identification conditions (M9 medium, arabinose, 37 °C) by ∼300-fold; ara, arabinose; glc, glucose.

Table 2. Structural Statistics for the Family of 15 Structures Selected To Represent the Solution Structure of Capistruin

restraining constraints	constraint violations
total: 169	distance violations, >0.5 Å: 0
distance, $i = j$: 88	rms deviations: 0.018 Å
distance, $\|i - j\| = 1$: 43	dihedral violations, >5°: 0
distance, $\|i - j\| > 1$: 27	rms deviation: 2.1°
dihedral: 8	average pairwise rms deviation (Thr^2−Phe^{18})
hydrogen bond: 3	backbone atoms: 0.15 Å
constraints/residue: 8.9	all heavy atoms: 0.52 Å

Our qualitative structure analysis was followed by a quantitative structure calculation on the basis of constraints obtained from NMR experiments. In this way, 158 distance constraints were obtained, with 47 for the backbone, 23 for long-range, and 88 for the side chains. The internal linkage was realized by setting a distance constraint between N of Gly_1 and Cγ of Asp_9 to 1.33 Å. Thus there were on average 8.3 distance constraints per residue.

The torsion angles ϕ were restrained to $-70 \pm 30°$ for Thr_2 and Phe_5 with $^3J_{HH\alpha} < 10$ Hz, and $-120 \pm 30°$ for Val_{12} and Ser_{14} with $^3J_{HH\alpha} \geq 10$ Hz. We thus established the conformation of the prochiral β-methylene protons and the range of the corresponding side chain torsion angle χ^1 for the following residues: Phe_5 (g^2t^3), Gln_6 (t^2g^3), Asp_9 (g^2g^3), and Ser_{14} (g^2t^3). For g^2t^3, t^2g^3, and g^2g^3 conformations around the Cα−Cβ bond, the torsion angle χ^1 was constrained in the range of 150 ± 30, -60 ± 30, and $60 \pm 30°$, respectively.

The calculation was initiated with 500 random conformers, and the resultant structures were engineered by the program package Sybyl 7.3[39] to include the covalent linkage between the nitrogen of Gly_1 and Cγ of Asp_9, followed by energy minimization under NMR constraints using TRIPOS force field within Sybyl. Thus, on the basis of low energies and minimal violations of the experimental data, a family of 15 structures was chosen. These 15 energy-minimized conformers show an average root-mean-square deviation (rmsd) for the backbone of 0.15 Å (Table 2) and are kept to represent the solution structure of capistruin.

Figure 4a shows the stereoview of the superimposed backbones of these 15 lowest energy structures, whose quality was

(39) *Sybyl7.3*; Tripos Inc.: 1699 South Hanley Rd., St Louis, MO 63144.

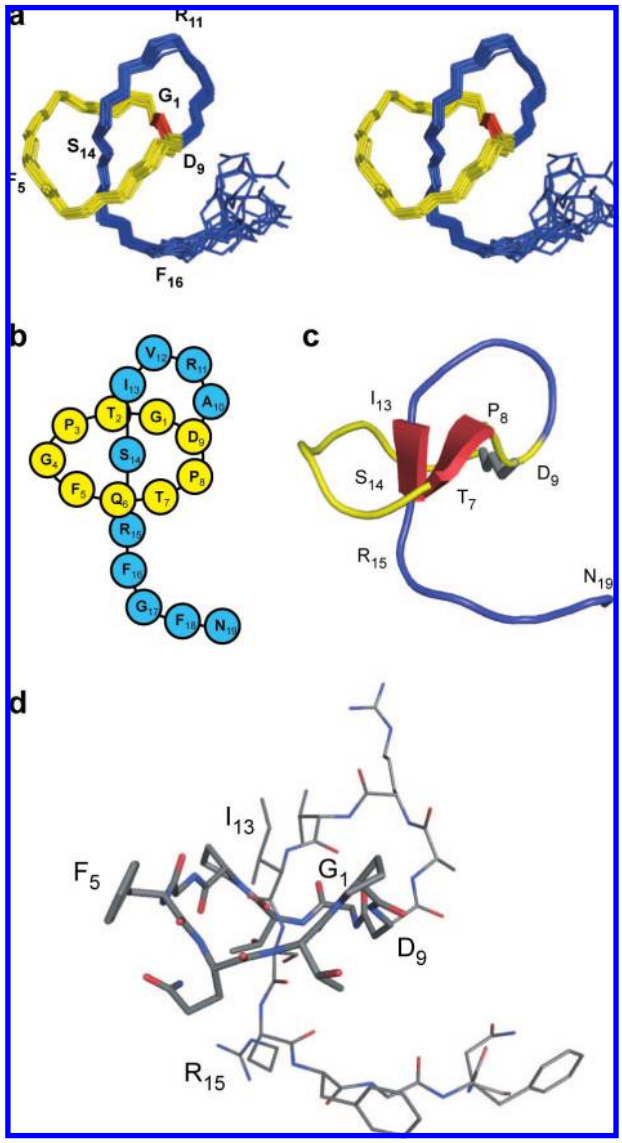

Figure 4. Capistruin structure in solution. (a) Superimposition of 15 lowest energy structures to represent the solution structure of capistruin shown in stereoview. Structures are superimposed over all backbone atoms. The isopeptide bond (red) between the α-amino group of G_1 and β-carboxy group of D_9 results in a macrolactam ring comprising residues G_1-D_9 (yellow) through which the C-terminal tail (blue) is threaded. (b) Schematic representation of capistruin structure in solution. (c) Ribbon representation of capistruin illustrating the main elements of secondary structure, a small antiparallel β-sheet (red) comprising residues T_7, P_8 and I_{13}, S_{14}, whereas S_{14} is located within the macrolactam ring (yellow, isopeptide bond shown in gray). (d) Representative structure of capistruin colored by elements. Macrolactam ring is highlighted. I_{13} and R_{15} are located above and below the macrocyclic ring, respectively.

evaluated using the PROCHECK-NMR program[40] (for a Ramachandran plot,[41] see Supporting Information Figure 4). The obtained structure clearly indicates that capistruin is a lasso peptide, where the C-terminal tail threads through the nine-membered ring. The backbone of the peptide adopts a very rigid fold, only the three C-terminal amino acids displaying a high grade of flexibility, as suggested by the absence of long-range NOEs in this region. The exocyclic C-terminal tail can be subdivided into three parts depending on the orientation toward the ring. Four residues, namely, Ala_{10}, Arg_{11}, Val_{12}, and Ile_{13}, are located above the macrolactam ring, while the very C-terminal residues Arg_{15}, Phe_{16}, Gly_{17}, Phe_{18}, and Asn_{19} are found below the cycle. Therefore, our initial hypothesis that Phe_{16} and Phe_{18} were assumed to be responsible for sterically trapping of the C-terminal segment can be ruled out.

Interestingly, Ser_{14} is located within the nine-membered ring (Figure 4b−d), which was confirmed by proton exchange studies in D_2O (Supporting Information Figure 5). The amide proton of Ser_{14} could not be exchanged after 10 days in D_2O. As shown in Figure 4c, the fold of capistruin is characterized by a small antiparallel β-sheet comprising Thr_7-Pro_8 and $Ile_{13}-Ser_{14}$, which is formed between a part of the ring and the threading C-terminal tail. The two β-strands are connected by a β-turn involving residues Asp_9-Val_{12}, which can be classified as a type I β-turn. The stability of these amide protons involved in intramolecular interactions against temperature is further confirmed by a series of variable temperature experiments (Supporting Information Figure 6). The main interactions stabilizing the lasso fold are van der Waals interactions of the amino acid side chains, which are predominantly hydrophobic in nature. A hydrophobic patch is present on the surface comprising the two proline residues Pro_3 and Pro_8 of the ring and the side chains of Val_{12} and Ile_{13}. Because of the macrolactam structure capistruin contains only three charges, namely, the guanidine groups of Arg_{11} and Arg_{15}, and the C-terminal carboxyl group, but these charges are not in close proximity, ruling out a further stabilization of the lasso fold of capistruin by the formation of salt bridges.

Heterologous Expression in *E. coli.* Generally, gene knockout studies or heterologous synthesis in a nonproducing strain are used to prove the necessity of genes for the production of a natural product of interest. For this purpose, the whole genetic system of capistruin was cloned into a pET-41a(+) vector, setting *capABCD* (~4.5 kb) under control of a T7 promotor and a T7 terminator, respectively (Figure 5a). Additionally the *capA* gene was translated from an artifical, vector-based ribosomal binding site (rbs), while for the translation of *capB*, *capC*, and *capD*, the intrinsic rbs from *B. thailandensis* E264 were used. The *E. coli* BL21(DE3) that was transformed with the plasmid pET41a(+)_*capABCD* was subjected to 48 h fermentation in M20 medium. Analysis of the culture supernatant revealed the successful heterologous synthesis of capistruin, as the exact mass could be observed in the induced cultures ($[M + 2H]^{2+}_{heterologous} = 1025.0212$; $[M + 2H]^{2+}_{calculated} = 1025.0191$; $[M + 2H]^{2+}_{B.\ thailandensis} = 1025.0206$) (Figure 5b). The heterologously produced capistruin showed the same retention time (19.76 min) as native capistruin (19.71 min) (Supporting Information Figure 7) and the same fragmentation pattern. No peptide was detected in noninduced cultures. The yield for the heterologous synthesis was 0.2 mg/L of culture, 30% compared to the natural host. Interestingly, we were not able to detect the lasso peptide in the supernatant of induced cells fermented in LB medium.

Antibacterial Activity of Capistruin. The antibacterial activity of capistruin was assessed against a series of Gram-positive and Gram-negative bacteria. *Burkholderia caledonica*, *E. coli* 363, and *Pseudomonas aeruginosa* AT27853 displayed the highest susceptibility to the peptide, with MIC values of 12, 25, and 50 μM, respectively (Supporting Information Table 2). The other *Burkholderia* strains tested were slightly susceptible to capistruin, with MIC values in the range of 100−150 μM. MccJ25

(40) Laskowski, R. A.; Rullmann, J. A. C.; MacArthur, M. W.; Kaptein, R.; Thornton, J. M. *J. Biomol. NMR* **1996**, *8*, 477–486.
(41) Laskowski, R. A.; Macarthur, M. W.; Moss, D. S.; Thornton, J. M. *J. Appl. Crystallogr.* **1993**, *26*, 283–291.

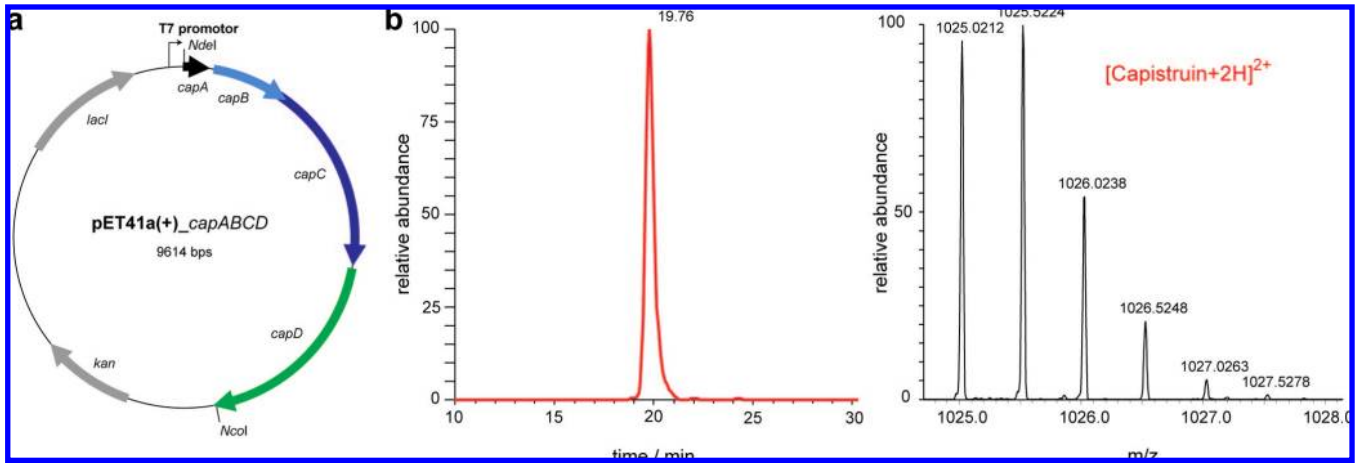

Figure 5. Heterologous expression of capistruin in *E. coli* BL21(DE3). (a) Map of the pET41a(+) derived plasmid used for heterologous expression of capistruin gene cluster in *E. coli* BL21(DE3). (b) LC-MS analysis of the supernatant of an *E. coli* BL21(DE3) strain transformed with pET41a(+)_*capABCD* shown as extracted ion chromatogram (EIC) and mass spectrum of capistruin produced by the engineered *E. coli* strain ($[M + 2H]^{2+}_{heterologous}$= 1025.0212; $[M + 2H]^{2+}_{calculated}$= 1025.0191, deviation 2 ppm).

was active against the *E. coli* and *Salmonella* strains tested, as already described,[18,42] but was revealed to be inactive against the *Burkholderia* and *Pseudomonas* strains tested here.

Discussion

Within the class of ribosomally assembled bioactive peptides, lasso peptides share a unique fold composed of a C-terminal tail entrapped within an 8/9-residue ring, thus providing increased stability combined with a diverse spectrum of biological activities. In this article, we predicted from the genome sequence that *Burkholderia thailandensis* E264 would produce a lasso peptide, and we were also able to identify a compound of the calculated mass in the culture supernatant. Mass spectrometric analysis verified its primary structure and ruled out a possible head-to-tail cyclization and a "normal" branched cyclic topology, suggesting that the peptide (capistruin) adopts a lasso fold. Optimized fermentation conditions considerably increased the production of capistruin and facilitated further structure elucidation by NMR spectroscopy, which finally proved the lasso structure. Furthermore, heterologous expression in *E. coli* was established, and biological activity studies revealed that capistruin displays antibacterial activity against closely related *Burkholderia* and *Pseudomonas* strains. To the best of our knowledge, this is the first example of a rationally based identification of a lasso peptide.

In nature, the production of secondary metabolites usually depends on the current growth conditions present in the habitat. Therefore, the discovery of natural products under laboratory conditions is clearly dependent on an effective simulation of this situation, as described for *Streptomyces* species by the OSMAC (one strain—many compounds) approach.[43] An interesting finding of this article is that capistruin production exemplifies this interdependence, as the growth conditions greatly influence the synthesis of the lasso peptide. Cultivation in M20 medium increased the production by 300-fold compared to our initial conditions and in the first place facilitated NMR structural studies. Surprisingly, the heterologous production of capistruin in *E. coli* was also successful only in M20 medium but failed in LB medium. This failed production may be caused by the susceptibility of the precursor protein CapA to proteolytic degradation, as described for the MccJ25 precursor protein McjA.[22,23] Certainly, an up to now unknown regulation mechanism on the transcriptional level of CapB, CapC, and CapD biosynthesis cannot be ruled out as another explanation for this finding. Surprisingly, capistruin is produced in the exponential phase, and synthesis arrests in the transition from late exponential phase to early stationary phase. This is in contrast to MccJ25 and also contrary to most antibiotics whose biosynthesis takes place when cells approach the stationary phase.[38,44] Therefore, capistruin production is not regulated by nutrient depletion as the common signal for stationary phase induction.

Developing a heterologous expression system of a biosynthetic gene cluster is an advantageous strategy compared to gene knockout studies. Due to genetic tractability of the heterologous host, it facilitates the straightforward design of natural product variants.[45] The successful heterologous production of capistruin in M20 medium demonstrates that the *capABCD* gene cluster is sufficient for the biosynthesis of capistruin and that the lasso peptide is released into the culture supernatant after intracellular biosynthesis in *E. coli*.

Mass spectrometric analysis of capistruin indicated a lasso fold of the molecule, as the poor fragmentation behavior and the observed y series of the C-terminus in MS^n experiments were not consistent with either a cyclic peptide (head-to-tail cyclization) or a branched cyclic peptide. The internal amide linkage between Gly_1 and Asp_9 was demonstrated by MS^3 experiments and further confirmed by strong NOEs between NH of Gly_1 and the side chain protons of Asp_9. Long-range NOEs between Hα or NH of the residues forming the nine-residue ring to side chain protons of the C-terminal tail indicated a threading of the tail through the ring. Structure calculation definitely proved capistruin to adopt the lasso fold. Generally, the lasso fold is characterized by a threading of the C-terminus through a ring generated by an internal amide linkage within the N-terminus. It raises the question of how this fold is stabilized or, generally speaking, how an unthreading is circumvented. In the case of MccJ25, the two bulky side chains

(42) Portrait, V.; Gendron-Gaillard, S.; Cottenceau, G.; Pons, A. M. *Can. J. Microbiol.* **1999**, *45*, 988–994.
(43) Bode, H. B.; Bethe, B.; Hofs, R.; Zeeck, A. *Chembiochem* **2002**, *3*, 619–627.
(44) Martin, J. F.; Demain, A. L. *Microbiol. Rev.* **1980**, *44*, 230–251.
(45) Chang, M. C.; Keasling, J. D. *Nat. Chem. Biol.* **2006**, *2*, 674–681.

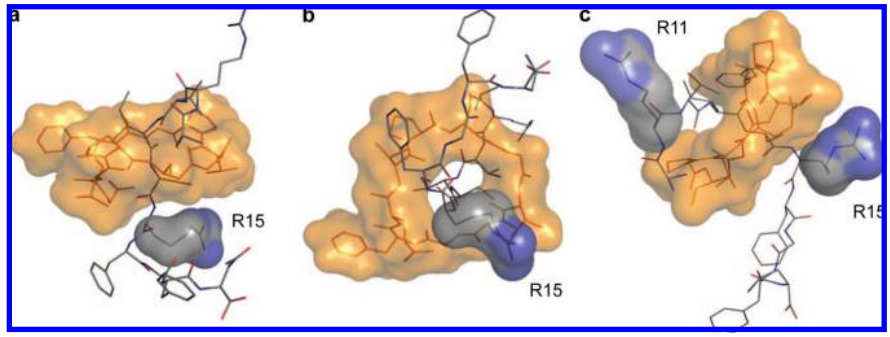

Figure 6. Interactions between the C-terminal tail and the macrocyclic ring. (a, b) Two orthogonal views of the threading of the C-terminal tail. The macrocyclic ring and its surface are shown in orange, and the side chain and surface of R15 are colored in blue and gray. Steric hindrance of the bulky side chain of R15 entraps the tail within the ring. (c) Location of R11 and R15 on opposite sides of the macrocyclic ring functioning as a plug from each side in MS fragmentation experiments.

of Phe_{19} and Tyr_{20} sterically trap the tail within the ring. Our initial hypothesis was that, in capistruin, Phe_{16} and Phe_{18} could fulfill this function. Interestingly, Arg_{15} is the first residue positioned below the cycle, whereas $Ala_{10}-Ser_{14}$ are located above and within the nine-residue ring, respectively. However, taking into account the bulkiness of an Arg side chain, Arg_{15} seems to be responsible for the sterically entrapping of the tail within the ring (Figure 6a,b).

It further explains the observed unusual fragmentation pattern. In MS^2 studies of the doubly protonated species of capistruin, we only observed y series of broken bonds C-terminally to Arg_{11}, but the cyclic nine-residue peptide fragment was not detected. It could only be observed upon MS^3 studies of the *m/z* 1110.7 fragment ion, representing the first 11 amino acids of capistruin (Gly_1-Arg_{11}). In consideration of the fact that Arg_{15} represents the plug of the lasso fold, Arg_{11} is functioning as a plug, but from the opposite side (Figure 6c). Therefore, a bond breakage N-terminally of Arg_{11} would result in a binary peptide complex consisting of a cyclic and a linear peptide, which is entrapped by the two bulky side chains of Arg_{11} and Arg_{15}. This binary complex cannot be distinguished from native capistruin in MS experiments.

Branched cyclic peptides are widespread in nature and can be synthesized by post-translational processing of ribosomal peptides as well as by thioesterase-mediated cyclization in nonribosomal peptides. To our knowledge, only two examples for ribosomal branched cyclic peptides are known, including MccJ25 and the herein presented capistruin. Interestingly, both peptides are not "normal" branched cyclic peptides, but adopt the complex three-dimensional lasso fold. Additional peptides containing a similar linkage have been discovered. However, the genome sequence of the producing strains is not accessible, and thus it is still not clear whether these peptides are of ribosomal or nonribosomal origin. These so far unclassified peptides include anantin,[12] RES-701-1,[46] MS-271,[47] and RP 71955[14] from *Streptomyces* species, propeptin[11] from *Microbispora*, and lariatin[9] from *Rhodococcus*. The three-dimensional structure was determined for several of these peptides (RES-701-1,[48] MS-271,[10] RP 71955,[14] and lariatin[9]), and all of them

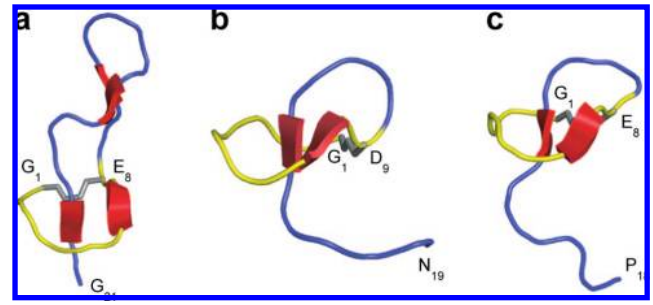

Figure 7. Comparison of the lasso peptide structures of MccJ25, capistruin, and lariatin. Ribbon representation of the lasso peptides MccJ25 (a), capistruin (b), and lariatin (c). All peptides share a macrocyclic ring (yellow) resulting from an isopeptide bond between the N-terminal glycine and an Asp/Glu side chain at position 8 or 9 (gray). The C-terminal tail is threaded through the ring, and the short antiparalell β-sheets (red) contribute to the stability of each molecule.

share the lasso structural motif, whereas MS-271 and RP71955 contain additional disulfide bonds and therefore belong to class I lasso peptides.[4] Although the representatives of class II lasso peptides (characterized by the absence of disulfide bonds) share a common primary structure and the lasso structural motif, they still display significant differences, as demonstrated by the structures of MccJ25, capistruin, and lariatin (Figure 7).

MccJ25 and lariatin consist of an eight-residue ring formed between the N-terminal Gly and the carboxyl group of Glu_8, whereas capistruin is composed of a nine-residue ring using the carboxyl group of Asp instead of Glu. The secondary structures of all of them are characterized by antiparallel β-sheets, formed between amino acids of the cycle and the threading tail. Additionally, MccJ25 displays another antiparallel β-sheet within the tail, forming a β-hairpin structure. In MccJ25, the tail is entrapped in the ring by Phe_{19} and Tyr_{20}. In capistruin, Arg_{15} is responsible for the trapping of the tail, whereas in lariatin, no such bulky side chain is located below the cycle. Comparing capistruin and MccJ25, a second bulky side chain like Phe_{19} in MccJ25 is most likely not necessary if the two β-strands formed by the cycle and the tail are connected by a short β-turn instead of a β-hairpin motif. The ring torsion of the β-turn circumvents a further passing of the tail through the ring and increases the rigidity of the structure.

The biological activity of lasso peptides is very diverse, ranging from the endothelin B receptor selective antagonist RES-701-1[46] to antimicrobial activity of MccJ25 and lariatin.[49] As found for MccJ25,[18,42] capistruin displayed an antibacterial activity against closely related strains, including all tested

(46) Morishita, Y.; Chiba, S.; Tsukuda, E.; Tanaka, T.; Ogawa, T.; Yamasaki, M.; Yoshida, M.; Kawamoto, I.; Matsuda, Y. *J. Antibiot.* **1994**, *47*, 269–275.
(47) Yano, K.; Toki, S.; Nakanishi, S.; Ochiai, K.; Ando, K.; Yoshida, M.; Matsuda, Y.; Yamasaki, M. *Bioorg. Med. Chem.* **1996**, *4*, 115–120.
(48) Yoshida, M.; Katahira, R.; Yamasaki, M.; Matuda, Y. *Prog. Biophys. Mol. Biol.* **1996**, *65*, PA115–PA115.

Burkholderia strains, *Pseudomonas aeruginosa* AT27853, and *Escherichia coli* 363. The observed MICs are in the range of 12−50 μM. Strains that were shown to be sensitive to MccJ25 were resistant against capistruin. The results clearly demonstrate that the spectrum of activity of capistruin and MccJ25 differs significantly, but both lasso peptides are targeted on closely related strains and therefore may function as a tool to gain advantage over competing bacteria within the same habitat. Nevertheless, the MICs of capistruin are 100-fold higher compared to MccJ25,[18] and further antibacterial tests are necessary to reveal more sensitive targets. As capistruin displayed antibacterial activity against *Burkholderia ubonensis* and *Burkholderia vietnamensis*, which belong to the *Burkholderia cepacia* complex (Bcc) causing opportunistic infections especially in people with cystic fibrosis (CF),[50] the other species of the Bcc should be a good starting point for future investigations.

In conclusion, capistruin is an antibacterial lasso peptide displaying a new mode of entrapping the C-terminal tail within an N-terminal macrolactam ring which characterizes the lasso fold. The isolation, structural characterization, and successful heterologous expression demonstrate the potential of the available genome sequences for the discovery of novel natural products. The established heterologous production will facilitate the synthesis of capistruin mutants and provide further insight into the key features determining the stability of the lasso fold and structure activity relationships. In general, the presented approach should be advantageous for prediction and isolation of new lasso peptides in the future.

Acknowledgment. We would like to thank Annette Michalski for her excellent support in establishing the purification protocol of the lasso peptide. We gratefully acknowledge financial support from the Deutsche Forschungsgemeinschaft (M.A.M.), the Fonds der Chemischen Industrie (M.A.M. and T.A.K.), and the Deutscher Akademischer Austauschdienst (M.A.M. and T.A.K.).

Supporting Information Available: Antibacterial activity of capistruin, growth phase regulation of capistruin biosynthesis, comparison of retention times of heterologously produced and native capistruin, DQF-COSY and NOESY spectra of the fingerprint region, Ramachandran plot of the 15 lowest energy structures, ^{1}H variable delay spectra in D_2O, ^{1}H spectra at variable temperatures, and assignment of ^{1}H signals of capistruin. This material is available free of charge via the Internet at http://pubs.acs.org.

JA802966G

(49) Iwatsuki, M.; Uchida, R.; Takakusagi, Y.; Matsumoto, A.; Jiang, C. L.; Takahashi, Y.; Arai, M.; Kobayashi, S.; Matsumoto, M.; Inokoshi, J.; Tomoda, H.; Omura, S. *J. Antibiot.* **2007**, *60*, 357–363.
(50) Mahenthiralingam, E.; Urban, T. A.; Goldberg, J. B. *Nat. Rev. Microbiol.* **2005**, *3*, 144–156.